

Spectral Radiative Properties of Open-Cell Foam Insulation

D. Baillis,* M. Raynaud,† and J. F. Sacadura‡

Institut National des Sciences Appliquées de Lyon, 69621 Villeurbanne CEDEX, France

A method to determine radiative properties of open-cell foam insulation is described. The spectral volumetric absorption and scattering coefficients and the spectral phase function are predicted from the dimensions and hemispherical reflectivity of particles that constitute the solid structure by applying to these particles a combination of geometric optics laws and diffraction theory. Three types of carbon foam of different porosities are studied. Particle dimensions and porosity can be obtained from microscopic analysis, but solid hemispherical spectral reflectivity is very difficult to obtain directly. It is determined by the Gauss method of linearization, applied to bidirectional spectral transmittance data obtained from an experimental device using Fourier-transform infrared spectroscopy. Results obtained from this approach are consistent. Good agreement is observed between the experimental results of transmittance and reflectance and the theoretically predicted values computed from the identified values of particle hemispherical reflectivity.

Nomenclature

b	= minimum thickness of strut (Fig. 1), m
b_{\max}	= maximum thickness of strut (Fig. 1), m
f_s	= fraction defined by the dimensionless relation (strut cross-sectional area)/(area inscribed in a triangle defined by vertices of the strut)
\bar{G}	= average geometric cross-sectional area of a particle, m^2
I	= spectral radiative intensity, $\text{W} \cdot \text{m}^{-3} \cdot \text{sr}^{-1}$
I_0	= spectral collimated radiation intensity incident onto the sample, $\text{W} \cdot \text{m}^{-3} \cdot \text{sr}^{-1}$
N_v	= number of struts per unit volume, m^{-3}
\tilde{n}	= refractive index
P	= phase function, dimensionless
P_d	= phase function of particles due to diffraction, dimensionless
P_r	= phase function corresponding to reflection, dimensionless
T_e	= experimental results of transmittance or reflectance, sr^{-1}
T_t	= theoretical results of transmittance or reflectance, sr^{-1}
α	= absorption coefficient, m^{-1}
β	= extinction coefficient, m^{-1}
δ	= porosity, dimensionless
θ	= polar angle
μ	= $\cos \theta$
ρ	= particle hemispherical reflectivity, dimensionless
σ	= scattering coefficient, m^{-1}

Subscript

λ	= monochromatic wavelength
-----------	----------------------------

I. Introduction

INSULATING foam consists of a highly porous but coherent solid material with a cellular structure. Heat transfer in such media occurs by conduction through the solid material (Fig. 1) and through the gas filling the pores, and by thermal radiation, which propagates through the structure. Even if analytical or numerical techniques are available to solve the coupled heat transfer problem in semitransparent media, some difficulty remains to determine the radiative properties of these porous materials.

This paper deals with prediction of radiative properties for open-cell foam insulation and its application to carbon foams. There are two main groups of methods to determine radiative properties of porous media: analytical determination using theoretical models,¹ such as the well-known Mie theory, and experimental methods.² The first group of methods is interesting because they contribute to a better understanding of the complex physical radiative phenomena occurring in these materials. Doermann and Sacadura³ have developed a prediction model for open-cell foam insulations that is more sophisticated than previous methods.^{4–6} To apply this new model to a foam sample, knowledge of parameters such as porosity, particle sizes, and radiative properties of the solid material is required. Particle dimensions and porosity can be obtained from microscopic analysis but solid hemispherical spectral reflectivities are very difficult to obtain directly, and so, these parameters must be determined experimentally. A parameter identification method is used to determine the unknown parameters and then to deduce carbon foam radiative properties. This method uses experimental results of transmittance and reflectance obtained for several measurement directions and for several measurement wavelengths. The experimental device uses Fourier-transform infrared spectroscopy (FTS-IR). Theoretical transmittance and reflectance are obtained from the Doermann–Sacadura³ predictive model.

First, a short review of predictive modeling of radiative properties is presented and the Doermann and Sacadura³ model is recalled. Then, the identification method used to determine the unknown parameters, such as hemispherical spectral reflectivity of solid material, is described. Finally, results obtained from the identification method are given. Radiative properties (extinction coefficient, scattering coefficient, and phase function) of three different types of foam of different porosities obtained by this approach are presented. The consistency of hemispherical reflectivity results for carbon and a comparison between theoretical transmittance values and experimental transmittance data for several directions and wavelengths permit validation of this approach. The last two parts are believed to be new contributions.

II. Predictive Model for Radiative Properties

The radiative properties of foam that are required for solving the radiative transfer equation are the spectral volumetric scattering and absorption coefficients and the spectral volumetric phase function. These depend on particle shapes and sizes and can be obtained from the radiative properties of particles forming the foam, by adding up the effects of all of the particles of different sizes.⁷ The foam structure is complex: The unit cell closely resembles a pentagon dodecaeder. Very few works appear to have been devoted to the prediction of radiative properties of foam thermal insulation. The authors are aware only of the following: Glicksman and colleagues^{4,5}

Received 5 October 1998; revision received 1 March 1999; accepted for publication 1 March 1999. Copyright © 1999 by the authors. Published by the American Institute of Aeronautics and Astronautics, Inc., with permission.

*Assistant Professor, Centre de Thermique; domino@cethil.insa-lyon.fr. Member AIAA.

†Professor, Centre de Thermique; raynaud@cethil.insa-lyon.fr.

‡Professor, Centre de Thermique; Jean-Francois.Sacadura@cethil.insa-lyon.fr.

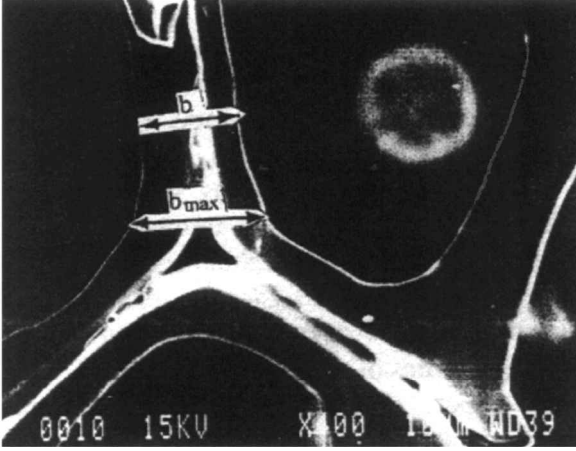


Fig. 1 Microscopic analysis of carbon foam sample (X400): Determination of dimensions b and b_{\max} .

considered the foam as a set of randomly oriented blackbody struts with constant thickness. They took an efficiency factor of one and neglected scattering phenomena by the struts.

Kuhn et al.⁶ used infinitely long cylinders to model the struts. They converted the triangular cross sections into circular ones with the same area. Then they used Mie scattering calculations to predict the radiative properties.

The Doermann–Sacadura model,³ which we use, represents an improvement over previous ones. Indeed, these authors have considered a particle modeling more representative of the actual geometry. It was obtained from the foam geometry description and from microscopic analysis of carbon open-cell foams (Fig. 1). Struts with varying thickness and strut junctures are considered. In common foams, four struts are connected making a strut juncture. So, if N_v is the number of struts per unit volume, there are N_v particles of type 1, which are struts; and $N_v/2$ particles of type 2, which are the strut junctures. The particles are assumed to have a random orientation and to be thick enough to be considered as opaque.

Moreover, these authors have taken into account scattering phenomena by applying to these particles a combination of geometric optics and diffraction theory. Indeed, when the particle size parameter $x = \pi d/\lambda$, where d is the particle diameter and λ is the wavelength, is much larger than one and when the refractive index \tilde{n} is not too small ($x|\tilde{n} - 1| \gg 1$), geometric optics combined with diffraction theory can be used to predict scattering behavior.⁷ The wavelengths considered are smaller than $15 \mu\text{m}$. Under these conditions $x \gg 1$ and $x|\tilde{n} - 1| \gg 1$ for the carbon foam studied. Application of these theories to the particles of the two types considered in the present study leads to the following results:

$$\beta_\lambda = 2N_v(\bar{G}_1 + \bar{G}_2) \quad (1)$$

$$\sigma_\lambda = (\rho_\lambda + 1)N_v(\bar{G}_1 + \bar{G}_2) \quad (2)$$

$$\alpha_\lambda = (1 - \rho_\lambda)N_v(\bar{G}_1 + \bar{G}_2) \quad (3)$$

where β_λ is the volumetric extinction coefficient, α_λ is the volumetric scattering coefficient, and α_λ is the volumetric absorption coefficient. G_j is the average geometric cross-sectional area of the particles of type j ($j=1, 2$) and ρ_λ is the spectral hemispherical reflectivity of particles.

The phase function obtained by adding the effects of the two types of particles is

$$P_\lambda(\theta) = \frac{\bar{G}_1 P_{1\lambda}(\theta) + (\bar{G}_2/2) P_{2\lambda}(\theta)}{\bar{G}_1 + \bar{G}_2/2} \quad (4)$$

where $P_{j\lambda}$ is the spectral phase function of particles of type j . This phase $P_{j\lambda}$ function resulting from the combination of geometric optics and diffraction theories can be expressed by the following relation:

$$P_{j\lambda}(\theta) = \frac{\rho_\lambda P_r(\theta) + P_{dj\lambda}(\theta)}{1 + \rho_\lambda} \quad (5)$$

where $P_{dj\lambda}$ is the spectral phase function due to the diffraction of particles of type j ; P_r is the phase function related to reflection. To determine $P_r(\theta)$, the following theorem⁸ is applied.

Theorem 1. The scattering pattern caused by reflection on a very large convex particle with random orientation is identical to the scattering pattern by reflection on a very large sphere of the same material and surface condition. The reflection is assumed to be diffuse. The phase function related to reflection from large, opaque, diffusely reflecting spheres is⁸

$$P_r(\theta) = (8/3\pi)(\sin \theta - \theta \cos \theta) \quad (6)$$

Moreover, a special emphasis has been placed by Doermann and Sacadura³ on taking into account the relations that describe the particle geometry in order to have the smallest possible number of parameters. Consequently, the radiative properties can be determined from the following parameters: b , b_{\max} , δ , ρ_λ , fs .

The details of this new prediction model for radiative properties require extensive explanations, which are given by Doermann and Sacadura.³ To quantify the improvement of their model, Doermann and Sacadura have presented results from numerical simulations. According to them, neglecting scattering is valid only for low-reflectivity solid material; otherwise the radiative conductivity difference between the current (complete) model and the model neglecting scattering can be as high as 21%.

To summarize, this new model represents a real improvement over previous work for the following reasons: Scattering is taken into account and particle modeling is closer to reality.

Until now, Doermann and Sacadura³ have presented results of their model from numerical simulation by considering different parameters, but the use of this model for a carbon foam sample requires the knowledge of the sample parameters. The parameters b , b_{\max} , and δ can be determined easily from microscopic analysis and photographs (Fig. 1). From Fig. 1, note that the minimum and maximum thickness of the strut can be measured more precisely and are easier to obtain than the mean cell diameter used as a parameter by Glicksman and colleagues.^{4,5} This is an advantage of the particle modeling taking into account the varying thickness of the struts. The main difficulty remains in the determination of ρ_λ and fs . In previous work,^{4,5} the fs value was taken as $\frac{2}{3}$, but from microscopic analysis of different foam samples, it can be observed that fs seems to vary significantly from one foam sample to another. The hemispherical reflectivity ρ_λ cannot be obtained from direct measurement because the material needs to be compacted for this measurement. Moreover, it cannot be obtained reliably from the literature because of the great dispersion of the reported data, and so, it has been preferred to determine ρ_λ and fs by using an identification method.

III. Parameter Identification

A. Method

This method uses experimental results of transmittances and reflectances, T_{eij} , obtained for several measurement directions i and for several measurement wavelengths j for a given set of samples; and theoretical transmittances and reflectances, T_{tij} , obtained for the same measurement directions and wavelengths as in the experiment and for the same samples. The T_{tij} are calculated using the Doermann–Sacadura³ predictive model with b , b_{\max} , δ , ρ_λ , and fs as parameters.

The goal is to determine the parameters fs and ρ_λ for nw wavelengths, which minimize the quadratic differences F between the measured and calculated transmittances over the N measurement directions and NL measurement wavelengths:

$$F(\rho_{\lambda 1}, \dots, \rho_{\lambda nw}, fs) = \sum_{j=1}^{NL} \sum_{i=1}^N [T_{tij}(\rho_{\lambda 1}, \dots, \rho_{\lambda nw}, fs) - T_{eij}]^2 \quad (7)$$

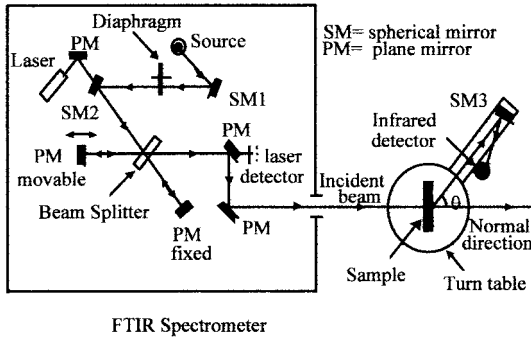


Fig. 2 Experimental device using FTS-IR to measure transmittance and reflectance.

The number of identified parameters is then $p = nw + 1$. The solid hemispherical reflectivities $\rho_{\lambda j}$ at the measurement wavelengths j are calculated from the nw parameters $\rho_{\lambda k}$, $k = 1, nw$ by linear approximation. We use the Gauss linearization method,⁹ which minimizes F by setting to zero its derivatives with respect to each of the unknown parameters. This nonlinear parameter estimation problem is solved iteratively. Typically $p = 8$, $N = 7$, and $NL = 134$ (Sec. IV). The ratio of the total number of measurements to the number of unknown parameters is 117. This ratio being large, the identification method is appropriate.

B. Experimental Setup

The experimental spectral transmittance data are obtained from an experimental setup that includes a Fourier-transform infrared spectrometer (FTS 60 A, Bio-Rad Inc.). The principle of the setup is shown Fig. 2. The source of radiation, characterized by a black-body emission spectrum at 1300°C, is a tungsten filament inside a silica tube. The radiation emitted by the source is modulated and enters nearly parallel onto the sample, with a divergence of half-angle θ_0 ($\theta_0 = 0.87$ deg). The detection system consists of a spherical mirror collecting the radiation and concentrating it on a linear detector (1.8–15.5 μm). It is mounted on a rotating arm, allowing measurement of the radiation transmitted or reflected by the sample at several angles. Both the spectrometer and the detection system are purged with dry air. The transmittances or reflectances $T_e(\theta, \lambda)$ for normal incidence are defined by

$$T_e(\theta, \lambda) = \frac{I(\theta, \lambda)}{I_0 d\omega_0} \quad (8)$$

where I is the transmitted or reflected intensity and I_0 is the intensity of the collimated beam normally incident onto the sample within a solid angle $d\omega_0$.

C. Theoretical Model

1. Analysis

Heat transfer in the experimental foam sample is calculated numerically. The boundary conditions and the assumptions are as follows: one-dimensional radiative transfer in the semitransparent medium, azimuthal isotropy, and omission of self-emission term because of the radiation modulation and phase-sensitive detection.

With these conditions the radiative transfer equation for the sample can be written in the following form:

$$\mu \frac{\partial I_\lambda}{\partial y} + \beta_\lambda I_\lambda = \frac{\sigma_\lambda}{2} \int_{-1}^1 I_\lambda(y, \mu') P_\lambda(\mu', \mu) d\mu' \quad (9)$$

where I_λ is the spectral intensity of radiation.

Foam spectral radiative properties used in the equation (coefficients of extinction β_λ , scattering σ_λ , and phase function P_λ) are determined by the predictive model of Doermann and Sacadura,³ which involves the unknown parameters ρ_λ and f_s .

The boundary conditions are

$$I_\lambda(0, \mu) = \begin{cases} 1 & \text{if } \mu_0 \leq \mu \leq 1 \\ 0 & \text{elsewhere} \end{cases} \quad (10)$$

$$I_\lambda(\ell_y, \mu) = 0 \quad \text{for } \mu < 0$$

2. Solution Method

The discrete ordinates method is applied to solve the integro-differential equation. Details of the solution have been reported by Nicolau.¹⁰ This solution, combined with the predictive model for radiative properties, permits determination of the theoretical transmittances and reflectances from the parameters δ , b , b_{\max} , ρ_λ , and f_s of the foam sample subjected to a collimated incident flux.

IV. Application to Carbon Foam

The identification method is applied to three different types of open-cell carbon foam.

A. Carbon Foam Data

The dimensional characteristics of the three types of carbon foam obtained from microscopic analysis are given in Table 1 with their uncertainties. For each type of foam, four specimen thicknesses were studied (Table 2).

1. Numerical Data

A quadrature over 24 directions is performed in the discrete ordinate method.¹⁰ The spherical space is discretized symmetrically into 12 directions each for the positive and negative μ . This quadrature is a combination of two Gauss quadratures. This method allows a concentration of ordinates in the neighbourhood of the normal direction, suitable for forward scattering materials ($\mu = 1, 0.999, 0.994, \dots$).

2. Measurement Data

Measurements cannot be obtained for all 24 integration directions because transmittance and reflectance values are too small for directions far from the normal to the sample. To overcome this problem, two transmittance measurements are used in the forward directions, for $\mu = 1$ and 0.999; and five reflectance measurements are used in the backward directions, for $\mu = -0.407, -0.638, -0.813, -0.915, -0.947$.

So, the number of measurement directions is $N = 7$. For each measurement direction, $NL = 134$ spectral transmittance or reflectance data have been selected in the wavelength range (2.04 $\mu\text{m} \leq \lambda \leq 15.34 \mu\text{m}$). Moreover, the sensitivity coefficient of f_s is the largest in the normal direction, $\mu = 1$, and decreases quickly when μ decreases. On the contrary, the sensitivity coefficient of hemispherical reflectivity is larger in the backward directions and the values are nearly the same in these backward directions.

3. Procedure

For each type j ($j = 1, 2, 3$) of foam, the following procedure is used.

Table 1 Data for three types of carbon foam

Foam type	$\delta \pm \Delta \delta$, %	$b \pm \Delta b$, μm	$b_{\max} \pm \Delta b_{\max}$, μm
1	97.50 ± 0.67	38 ± 4	60 ± 4
2	98.75 ± 0.44	34 ± 3	52 ± 4
3	98.2 ± 0.78	84 ± 7	125 ± 12

Table 2 Specimen thicknesses for the three types of carbon foam

Foam type	Specimen thickness, mm			
	Sample 1	Sample 2	Sample 3	Sample 4
1	3.06 ± 0.04	3.08 ± 0.04	4.04 ± 0.04	4.02 ± 0.04
2	3.98 ± 0.04	4.30 ± 0.04	4.96 ± 0.04	4.92 ± 0.04
3	7.04 ± 0.04	7.06 ± 0.04	7.76 ± 0.04	8.12 ± 0.04

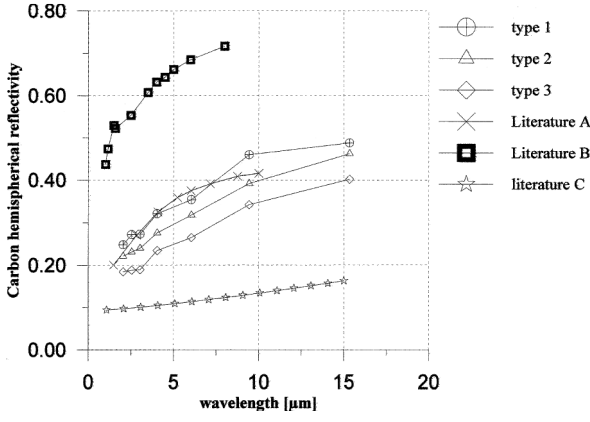


Fig. 3 Carbon hemispherical reflectivity: Comparison of results obtained from identification method for each type of foam with results from literature (A, measurement Ref. 11); B, theoretical calculation (Ref. 11); and C, calculated from optical constants (Ref. 12).

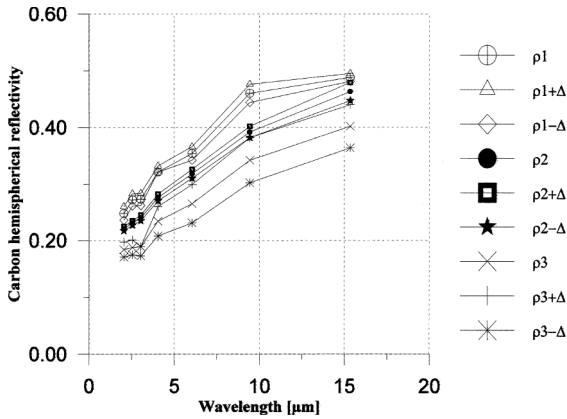


Fig. 4 Identified carbon hemispherical reflectivity for the three foam types.

For each of the four specimens ($i = 1, \dots, 4$), five experiments ($k = 1, \dots, 5$) have been performed to calculate the average transmittances and reflectances $\overline{T}_i(\theta, \lambda)$ and the mean square deviations $\Delta_i(\theta, \lambda)$ due to experimental errors.

$$\overline{T}_i = \frac{1}{5} \sum_{k=1}^5 T_{ki} \quad (11a)$$

$$\Delta_i = \frac{1}{\overline{T}_i} \sqrt{\frac{1}{4} \sum_{k=1}^5 (T_{ki} - \overline{T}_i)^2} \quad (11b)$$

For each specimen i of different thickness, the fraction $f s_i$ and the hemispherical reflectivity $\rho_{\lambda k, i}$ are identified from the average transmittances and reflectances, $T_{ei} = \overline{T}_i$ by using the parameter identification method described in Sec. 3.

Then these results, $(\rho_{\lambda k, i}, f s_i)$, are used to calculate the average over the four specimens, which allows one to obtain the value of the hemispherical reflectivity $\rho_{\lambda k}$ and the fraction $f s$ corresponding to the foam carbon studied. The mean square deviation of the identified values $(\rho_{\lambda k}, f s)$ also is calculated.

From these average identified values introduced in the radiative transfer model, theoretical transmittances and reflectances are obtained, which then can be compared with the experimental ones ($T_{ei} = \overline{T}_i$).

4. Identified Parameters $f s$ and $\rho_{\lambda k}$

The estimated $f s$ values for each type of foam are given in Table 3. In previous work,^{4,5} the $f s$ value was taken as a constant

Table 3 Estimated $f s$ values for the three types of carbon foam

Foam type	$f s \pm \Delta$
1	0.57 ± 0.011
2	0.335 ± 0.008
3	0.396 ± 0.025

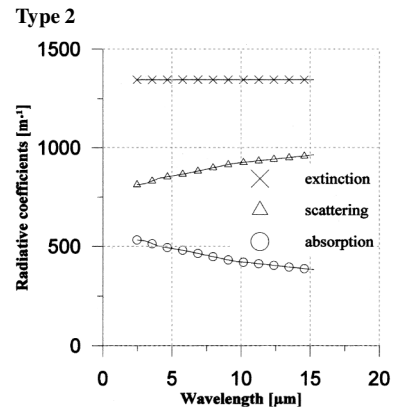
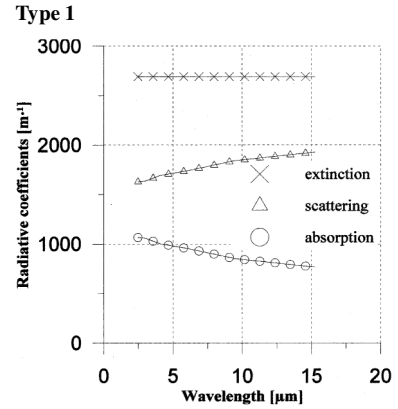
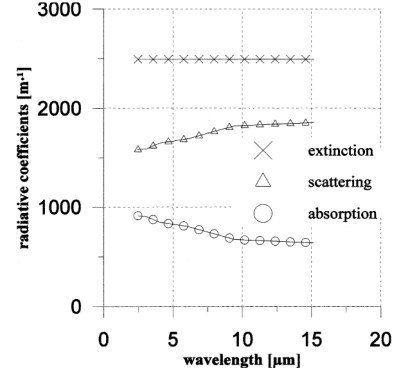


Fig. 5 Radiative coefficients of carbon foam by type of foam.

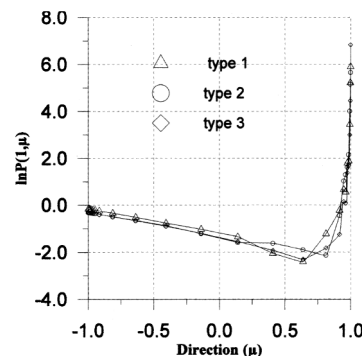


Fig. 6 Natural logarithm of phase function for the 10.07-μm wavelength for the three types of foam.

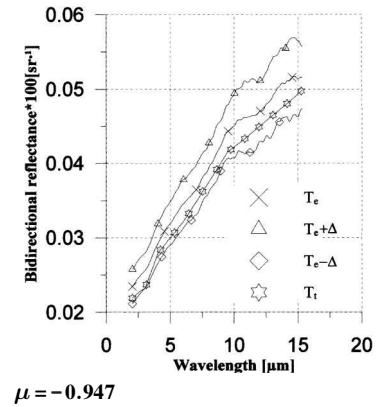
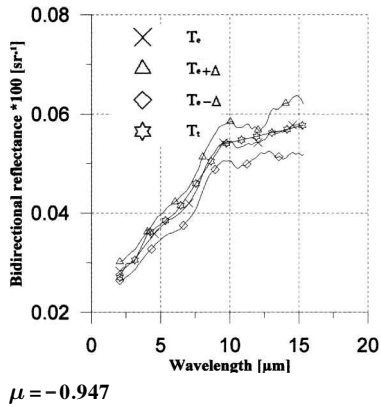
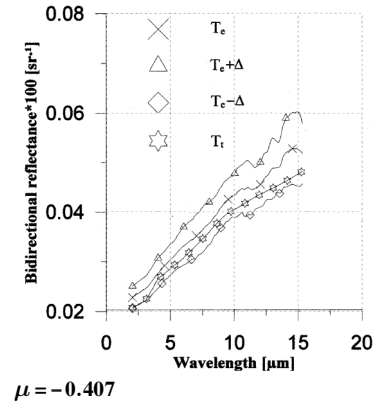
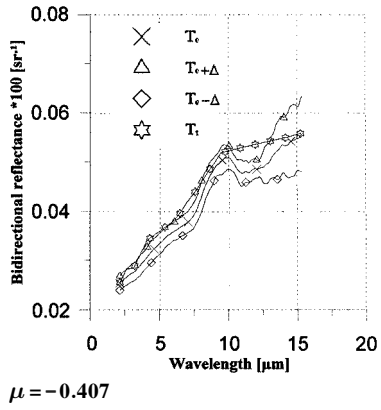
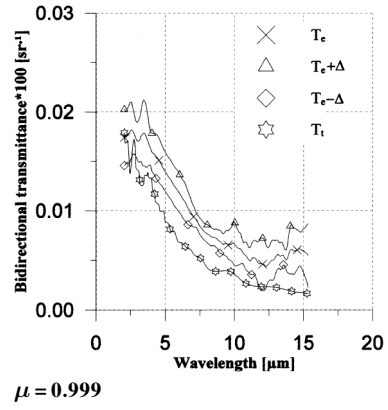
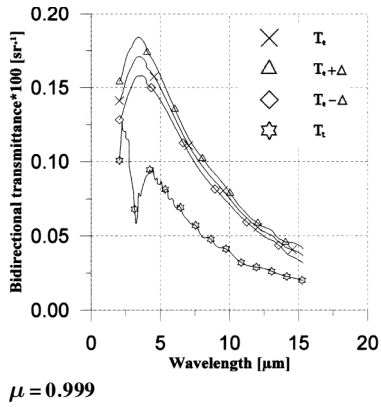
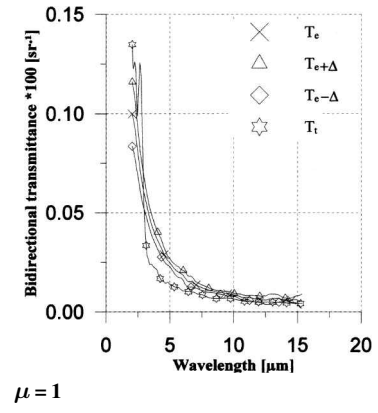
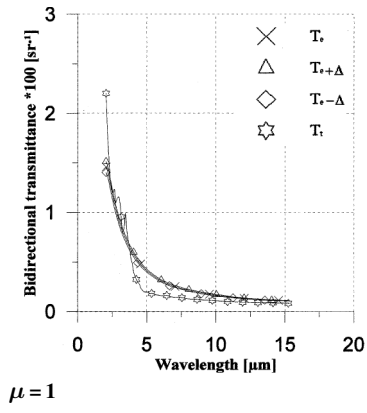


Fig. 7 Transmittance or reflectance results, defined by Eq. (8), for type 1 carbon foam sample of 4.02-mm thickness for normal incidence and different measurement directions (experimental results T_e ; plus or minus the standard deviation $T_e \pm \Delta$; and theoretical results T_t).

Fig. 8 Transmittance or reflectance results, defined by Eq. (8), for type 2 carbon foam sample of 4.92-mm thickness for normal incidence and different measurement directions (experimental results T_e ; plus or minus the standard deviation, $T_e \pm \Delta$; and theoretical results T_t).

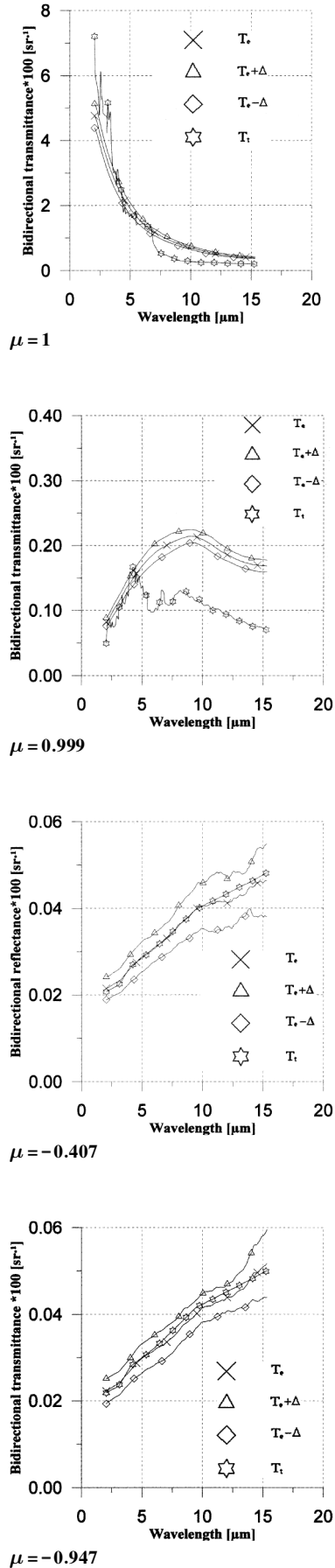


Fig. 9 Transmittance or reflectance results, defined by Eq. (8), for type 3 carbon foam sample of 8.12-mm thickness for normal incidence and different measurement directions (experimental results T_e ; plus or minus the standard deviation, $T_e \pm \Delta$; and theoretical results T_t).

equal to $\frac{2}{3}$. For the foam of type 1, the fs value is near $\frac{2}{3}$ but that is not the case for the foams of types 2 and 3. This means that, for different porosities and particle dimensions, the fs value varies. This confirms the microscopic analysis.

Seven parameters $\rho_{\lambda k}$, $k = 1, \dots, 7$, corresponding to the solid-material hemispherical reflectivity values at seven wavelengths are determined. This choice of $nw = 7$ represents a good compromise between speed and accuracy of calculation. The carbon spectral reflectivities determined from the measurements made on the four samples for each type of foam are shown in Fig. 3. They are compared with carbon reflectivity data obtained from the literature. An agreement can be observed. The reflectivities and mean square deviations are given in Fig. 4 for each type of foam.

5. Results for Radiative Properties of Foam

The spectral radiative properties for each type of foam, calculated from the previously identified values using the Doermann–Sacadura³ predictive model, are shown in Fig. 5. It can be seen that the extinction coefficient of foam of type 3 is smaller than that for the other types. The extinction coefficient is not a function of the wavelength; this is due to the combination of geometric optics laws and diffraction theory. Application of these theories to the particles considered in this study leads to Eq. (1). It can be deduced from this equation that the extinction coefficient is not a function of the wavelength. Moreover, from Brewster,⁷ it is clear that Mie theory results approach a constant extinction coefficient in the geometric optics region (large particle size). Further, note that Glicksman and colleagues, theory^{4,5} also leads to a constant extinction coefficient.

The natural logarithm of the phase function, $\ln P(\mu' = 1, \mu)$, is shown as a function of the scattering direction, μ , for the 10.07- μm wavelength for each type of foam (Fig. 6). These values are similar for all types of foam. A highly forward-peaked scattering is observed that is similar to the case of fibrous media described by Nicolau et al.²

6. Comparison of Theoretical and Experimental Results of Transmittance and Reflectance

For all of the samples of different thicknesses and types, the theoretical and experimental results of transmittance and reflectance are compared. Experimental and theoretical results are in good agreement. Only results for three samples are shown: type 1 of 4.02-mm thickness (Fig. 7), type 2 of 4.92-mm thickness (Fig. 8), and type 3 of 8.12-mm thickness (Fig. 9). Theoretical results are obtained from reflectivities and fs values corresponding to each type of foam. These values are calculated from the average of identified result for different thickness specimens of the same foam type. Experimental results plus or minus the standard deviations also are shown. Results are given for four measurement directions: $\mu = 1$; 0.999; -0.407 ; -0.947 . Note that the value of transmittance for incident direction ($\mu = 1$) is always much larger than its values in the other directions. For the forward direction $\mu = 0.999$, theoretical transmittance values are smaller than the experimental ones. This is probably due to the low sensitivity of the fs coefficient in this direction. Theoretical results of reflectance are within the range of experimental results.

V. Conclusion

A method to determine radiative properties of open-cell foam insulation is described. An identification method is employed that uses a predictive model for radiative properties and an experimental device based on a Fourier transform infrared spectrometer. The predictive model developed by Doermann and Sacadura³ was adopted. It is more sophisticated than previous models. The use of this model for foam samples requires the knowledge of several parameters. The three parameters b , b_{\max} and δ can be easily obtained from microscopical measurements, but the fraction fs and the solid-material, spectral hemispherical reflectivity are more difficult to determine. This is why an identification method was used.

An application of this methodology to three types of foam of different porosity and particle dimensions is presented. Radiative properties are given for the three types of foam. It was verified that

experimental and theoretical results of transmittance and reflectance obtained from the identified values are in good agreement. This study indicates that a good description of the foam geometry and inclusion of the scattering phenomena in the predictive model allows calculation of the spectral radiative properties of open-cell foam insulation.

References

- ¹Cunnington, G. R., and Lee, S. C., "Radiative Properties of Fibrous Insulations: Theory Versus Experiment," *Journal of Thermophysics and Heat Transfer*, Vol. 10, No. 3, 1996, pp. 460–465.
- ²Nicolau, V. P., Raynaud, M., and Sacadura, J. F., "Spectral Radiative Properties Identification of Fiber Insulating Materials," *International Journal of Heat and Mass Transfer*, Vol. 37, Suppl. No. 1, 1994, pp. 311–324.
- ³Doermann, D., and Sacadura, J. F., "Heat Transfer in Open Cell Foam Insulation," *Journal of Heat Transfer*, Vol. 118, No. 1, 1996, pp. 88–93.
- ⁴Glicksman, L. R., and Torpey, M. R., "A Study of Radiative Heat Transfer Through Foam Insulation," Rept. 19X-09099C, Massachusetts Inst. of Technology, Cambridge, MA, Oct. 1988.
- ⁵Glicksman, L. R., Marge, A. L., and Moreno, J. D., "Radiation Heat Transfer in Cellular Foam Insulation," *Developments in Radiative Heat Transfer*, Vol. 203, Heat Transfer Div., American Society of Mechanical Engineers, 1992, pp. 45–54.
- ⁶Kuhn, J., Ebert, H. P., Arduini-Chuster, M. C., Büttner, D., and Fricke, J., "Thermal Transport in Polystyrene and Polyurethane Foam Insulations," *International Journal of Heat and Mass Transfer*, Vol. 35, No. 7, 1992, pp. 1795–1801.
- ⁷Brewster, M. Q., *Thermal Radiative Transfer and Properties*, Wiley, New York, 1992, pp. 301–336.
- ⁸Van de Hulst, H. C., *Light Scattering by Small Particles*, Wiley, New York, 1957, pp. 103–113.
- ⁹Beck, J. V., and Arnold, K. J., *Parameter Estimation in Engineering and Science*, Wiley, New York, 1977, Chap. 7.
- ¹⁰Nicolau, V. P., "Identification des Propriétés Radiatives des Matériaux Semi-Transparents Diffusants," Ph.D. Dissertation, Dept. Thermique Énergétique, Institut Nationale des Sciences Appliquées, Lyon, France, Jan. 1994.
- ¹¹Autio, G. W., and Scala, E., "The Normal Spectral Emissivity of Isotropic and Anisotropic Materials," *Carbon*, Vol. 4, 1966, pp. 13–28.
- ¹²Boulet, P., "Etude du Transfert par Rayonnement à Travers les Milieux Fibreux," Ph.D. Dissertation, Dept. Mécanique et Énergétique, Univ. de Nancy, Nancy, France, Dec. 1992.